



Utilization of Hydrophobic Aerogel Sorbents Fabricated from Plastic Waste for Oil Contaminated Water Treatment



CrossMark

Sara S. Selim ^{a*}, Doaa I. Osman ^a, Sayed K. Attia ^a, Atef S. Darwish ^b, Renee I. Abdallah ^a, Ahmed I. Hashem ^b

^a Egyptian Petroleum Research Institute, Evaluation and Analysis Department, Nasr City, 11727 Cairo, Egypt

^b Department of Chemistry, Faculty of science, Ain Shams University, 11566 Cairo, Egypt

Abstract

This investigation describes a feasible, simple modification of the thermally induced phase separation technique to produce long-lasting oil aerogel sorbents from plastic waste (low-density polyethylene waste bags, high-density polyethylene waste bottles, and polypropylene waste containers). Numerous analysis, such as bulk density and porosity determination, XRD, FTIR, SEM, AFM, contact angle, and further practical experiments, were employed to detect the physical, structural, textural, morphological, topographs, and surface wettability aspects of the entire generated aerogels. Different samples contaminated with crude oil, diesel, and, lubricating oil were utilized to evaluate the generated aerogels' sorption capacities, removal efficiency, durability, recyclability, and stable sorption-desorption cycles. It's interesting to note that polypropylene aerogel derived from plastic waste has the highest sorption capacities (210%), removal efficiencies (99%), stable sorption-desorption cycles (7 cycle), and long lifespan of other materials. This is due to its high water contact angle (148°), hierarchical rough surface, superior porosity with polymodal pore geometries, and intrinsic stereo structures. With limited stability and reusability, both aerogels made from waste low-density and high-density polyethylene exhibit reduced oil absorption capacity and removal efficiency for all types of oil.

Keywords: Plastic waste; aerogel; polyethylene; polypropylene; adsorption; oil spill; water treatment.

1. Introduction

Turning plastic garbage into aerogel sorbents with unique qualities and multiple applications through simple procedures is a creative solution to a major problem, as per the circular economy approach. It is an important objective to find cost-effective, durable, and environmentally sound solutions to the problems of oil spills and the buildup of plastic trash. Water shortage, hydrological event variability, competitiveness and battle over water resources, and poor water quality are the main factors driving human efforts to minimize, treat, and reuse waste water these days [1]. A discharge of liquid hydrocarbons, often known as an oil spill, could result in serious long-term risks in all areas, including ecological, maritime, public health, social, economic, and communal considerations. [2]. The International Federation of Cruise Ship Pollution estimates that, due to the five million tons of oil that are transported worldwide each year, about 47,000 tons of oil derivatives are released into the ocean on a big scale at a pace of 53 times between 2010 and 2017 [3,4]. Between 1962 and 1997, there were about 826 oil leak incidents reported in the United States, resulting in the loss of 1.02 x 10⁶ tons of crude oil. Furthermore, the Erika oil spill in 1999 and the Mexcio Gluf oil leak in 2010 both resulted in major economic and environmental consequences [5]. A ton of oil spilled into the ocean causes an oil layer to spread on the surface of the ocean around 12 km² in area. This oil layer has detrimental consequences on the ecology, physics, and chemistry [4]. Because an oil spill would discharge heavy metals, polycyclic aromatic compounds, blue green algae, and disagreeable odors into the water, it would therefore have a negative impact on aquatic life, agriculture and irrigation, human health, and tourism. Therefore, the deterioration of food, water, and air would lead to the spread of human diseases like cancer. In addition, some oil components e.g. polynuclear aromatic hydrocarbons are known to be carcinogenic and mutagenic. A wide range of weathering processes, such as spreading, dissolving, drifting, dispersion, evaporation, photolysis, biodegradation, agglomeration, the formation of water-oil emulsions, and adsorption onto colloids, are also involved after an oil leak occurs in a marine environment and continue throughout any treatment [6].

Traditional methods of remediation, including burning, common chemical treatments (solidifiers and dispersants), biological remediation (microbial treatments, biological reducing agents), and adsorption using commercial sorbents (polyurethane and polypropylene), proved to be ineffective due to their high cost and tendency to produce secondary pollutants [3,5,7,8]. Though subsequent oil spills have prompted research into more practical, affordable, and quick technologies [3], adsorption remains the most practical option due to its ease of use, efficiency, and cost-effectiveness [4].

*Corresponding author e-mail: bdalhlmysart@gmail.com; (Sara S. Selim).

Received date 02 August 2024; Revised date 01 September 2024; Accepted date 16 September 2024

DOI: 10.21608/ejchem.2024.308250.10102

©2025 National Information and Documentation Center (NIDOC)

Usually, sorbents come from synthetic, natural, or inorganic sources. These include clays, minerals, biosorbents, resins and polymers, activated carbons, nanoparticles, minerals and clays, and composites. In particular, a variety of sorbents have been investigated including modified natural materials [9], activated carbon [10], carbon nanotubes [11], carbon aerogels and xerogels [12], zeolitic imidazolate frameworks [13], cellulose based sorbents [14], virgin polymers, and waste plastic [5]. Nonetheless, bio-sorbents like peat, cotton, and wool exhibit three times the sorption capacities of commercial sorbents; also, they are not economically viable and their waste products (such as rice straw and stalks) are hydrophilic, meaning they have a limited surface area and poorer efficacy [15]. Activated carbon (AC) and biochar both have a large surface area and a highly porous structure; however, biochar requires surface modification due to the hydrophilic surface functional groups, whereas AC is more expensive [4, 16].

Natural polymers have been considered as potential effective sorbents due to their exceptional properties, which include low cost, non-toxicity, biodegradability, biocompatibility, tunable surface properties, and mechanical stiffness [17]. Their disadvantages include their low purity and selectivity, the hydrophilic groups they contain, the high cost of production. On the other hand synthetic polymers are not biodegradable [18]. Inspired by the natural super-wetting phenomena, such as the surfaces of lotuse leaves that are naturally super hydrophobic and the surfaces of frogs and desert beetles that are naturally super hydrophilic, artificially superhydrophobic surfaces have been designed and fabricated in a variety of three-dimensional morphologies, including foams, sponges, and aerogels, which are superoleophilic materials [19]. Despite having a high surface area, a variable design, and low function costs, polyurethane foams are not recyclable and have hydrophilic groups (amino and carboxylic groups) that reduce their efficiency [19].

Aerogels are distinct phase materials with exceptional properties such as extremely low density, high porosity, high surface area, and ultra light weights (90–99% air). They are used as a safe, affordable, sustainable, and easy-to-use materials for absorbing spilled oil and other contaminants [5]. Several based aerogels have been employed in waste water treatment, including chitosan, cellulose, gelatin, alginate, charcoal, metal oxide frame work (MOF), silica, carbon [1]. Approximately 400 million tons of plastic polymers are created and then disposed each year. Consequently, it is estimated that by 2050, almost 1100 million tons of plastic waste (PW) would be produced [20]. According to ecological and economic perspectives, over 13% of the anthropogenic soil wastes account for PW, which has accumulated astonishingly over time and is haphazardly disposed of in billions of tons in ecosystems including rivers, seas, farms, and coastal areas [21,22]. Using mechanical and chemical recycling techniques, just 10% of produced PW is recycled [22]. However, traditional methods of treatment, such as incineration and landfills, squander the material and energy value and have other detrimental ecological effects [21]. It is noteworthy that a major issue lies in the conversion of PW (low-density poly ethylene (LDPE), high-density poly ethylene (HDPE), and poly propylene(PP)) into PW aerogel sorbents [5]. By solvent extraction, high molecular weight polyethylene (HMW PE) was converted into PE aerogel sorbent, which absorbed 180% of its initial weight oil [23]. Furthermore, rubber latex coated with superhydrophobic HDPE aerogel was created and studied for oil-water separation [24].

The sorptive oil removal of PW-derived LDPE aerogel with different modifications has only recently been studied in a limited number of investigations [20]. For selective oil sorption, HDPE aerogel from PW bottles has been mixed in other investigations with its high molecular weight virgin polymer [25]. Moreover, Gan et al. [26] synthesized an HDPE aerogel membrane from trash and utilized it for oil/water emulsion separation. It was also reported that waste HDPE bottles could potentially be used to create selective oil sorbent films [27]. Lang et al. [28] also prepared a superhydrophobic PP aerogel coated polyurethane sponge for oil and water separation. In this context, a NaCl cavity agent was used to construct a trimodal PP oil sorbent film from waste using spin coating [21]. Additionally, a modified aerogel surface containing PP and a carboxy methyl cellulose composite with methyltrimethoxysilane was fabricated and applied to heat insulation and oil spill remediation [29]. To our knowledge, there is no previous work comparing the topological, structural, and physical characteristics of PW aerogels (including PP, HDPE, and LDPE) or how well they absorb different types of oil. It is imperative that this research gap be identified and thoroughly examined.

So, we wish to report here on the first comprehensive analysis comparing the prepared PW LDPE, PW HDPE, and PW PP aerogels as effective oil-absorbing sorbents derived from PW. The produced PW aerogels' physical, structural, textural, surface morphology and topology, and surface wetting behavior have all been studied. Ultimately, it was found that the created PW PP aerogel has superiority over PW HDPE and PW LDPE due to its structural and topological characteristics, which induce its ability to remove oil as much as possible, its long-term sorption/desorption cycle, its mechanical durability, and its ease of regeneration.

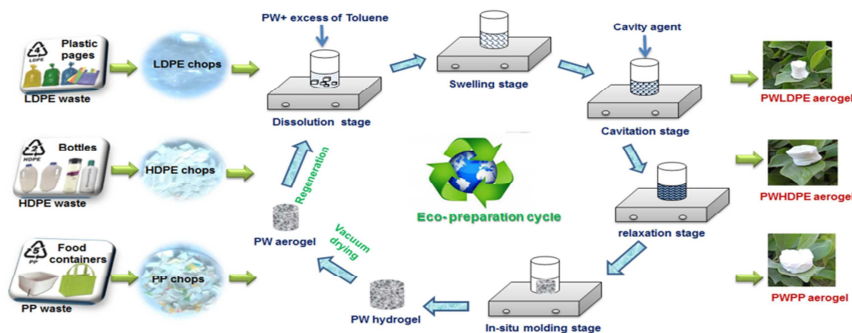


Figure 1: Eco- preparation cycle of plastic waste derived aerogels.

2. Experimental section

2.1. Preparation of waste derived aerogels

As part of the circular economy strategy, Fig.1 shows the cycle of PW aerogels' preparation from plastic trash by facile modified thermal induced phase separation technique (TIPS). In general, the following steps were followed to prepare all PW aerogels: (1) solvent dissolution; (2) swelling; (3) structural cavitation; (4) relaxing; (5) molding; (7) drying; and (8) washing. To put it precisely, 1g of each type of shredded plastic waste (LDPE, HDPE, and PP) is dissolved in the appropriate volume of toluene at the polymer melting point in a convenient beaker. Following its dissolution, it swelled and is subsequently mixed violently with 10% sodium carbonate. After that, phase-induced separation is allowed to occur. Following that, the hydrogel is cooled and vacuum-dried at 80 °C to produce the PW aerogel.

2.2. Characterization of waste derived aerogels

2.2.1 Bulk density and porosity

The waste-derived aerogels' bulk densities (ρ_{bulk}) were calculated by measuring the weight to displacement volume ratio for each sample's pre-mass center component in a measurable cylinder glass filled with water according to the following formula

$$\rho_{\text{bulk}} = m/v$$

where m and v stand for the masses (g) and water volume displacement (ml), respectively, of the aerogels.

Using the measured bulk density values (ρ_{bulk}) and the skeletal density values (ρ_{skeletal}) of every waste (LDPE, HDPE and PP), the porosity percent (P %) of every waste derived aerogels is determined according to the following equation:

$$P (\%) = (1 - \rho_{\text{bulk}}/\rho_{\text{skeletal}}) \times 100$$

2.2.2 Powder X-ray diffraction (XRD) measurements

Powder X-ray diffraction (XRD) measurements were performed for grounded portion of the prepared aerogels using an X'Pert PROP Analytical apparatus equipped with CuK α radiation ($k = 0.1541$ nm) at range of $4^\circ < 2\theta < 90^\circ$. The crystallite sizes of the crystalline portions were calculated every aerogel using the Scherrer equation, which is expressed as $D_{\text{hkl}} = k\lambda / B_{\text{hkl}} \cos\theta$, where D_{hkl} , hkl , K , λ , B_{hkl} , and θ represent the crystallite size in the direction perpendicular to the lattice planes, the Miller indices of the planes being analyzed. A numerical factor frequently referred to as the crystallite-shape factor, the wavelength of the X-rays, the width (full-width at half-maximum) of the X-ray diffraction peak in radians, and the Bragg angle, respectively were determined.

2.2.3 Fourier Transform Infrared (FTIR) spectroscopy

Using a Perkin Elmer spectrometer model 100 series, the synthesized aerogels were examined using FTIR in the 400-4000 cm^{-1} range to determine their functional groups.

2.2.4 Field Emission Scanning Electron Microscopy (FESEM)

FESEM analysis was performed on the entire synthesized aerogel samples to determine their microstructure, morphology, surface roughness, and topology using JMS – IT 200 at 10 kV with magnification of $\times 10,000$ and resolution of 512×383 .

2.2.5 Atomic Force Microscopy (AFM)

Two dimensional and three dimensional topographs of the produced PW aerogels were investigated using Flexxciem Nanosurf Dynamic Mode NCLR Cauntilerer. Furthermore, the surface roughness degree of them was indicated.

2.2.6 Water contact angle (WCA) measurement

WCA analysis was done to ascertain the wettability of all of the prepared aerogels using Attention Theta Optical Tensiometer (BioInScientific Company, Finland).

2.2.7 Water repellency study

For one week, each preweighted aerogel was submerged in 200 milliliters of water to guarantee that the synthesized aerogel samples had an intrinsic water-repellent quality. A daily weigh-in was obtained in order to determine the total amount of water adsorbed during the dipping period.

2.3 Oil spillage sorption capacity and removal efficiency

To test the produced PW aerogels' potential to absorb and remove various types of oil from seawater, a variety of oils, including crude oil, diesel, and lubricating oil, were employed. To be exact, 100 ml of the prepared saline water was introduced into 250 ml beaker, and 2 g of each oil was dumped into it. After being submerged in oil for half an hour, each PW aerogel was held in the air to allow any extra oil to drain off the surface. Prior to and following each test, the used PW aerogel was weighed. Every sorption run was performed at least three times, and the final results were calculated by correcting the average readings. The following formulas are used to calculate both the sorption capacity and the removal efficiency (Wt%):

$$\text{Sorption Capacity (Wt.\%)} = (W_f - W_i) / W_i \times 100 \quad \text{Eq. (1)}$$

The sorption capacity (Wt.%) indicated the weight percentage of the sorped oil to original weight of PW aerogel. W_i and W_f , respectively, stand for the PW aerogel weights prior to and after the sorption test.

$$\text{Removal Efficiency (Wt.\%)} = W_r / W_i \times 100 \quad \text{Eq. (2)}$$

The removal efficiency specifies the weight percentage of the oil collected by the PW aerogel versus the total amount of oil spilled. W_t is the total amount of the oil spills under investigation, and W_r is the amount of oil removed after each run.

3. Results and Discussion

3.1 Characterization of the prepared aerogels derived from plastic wastes (LDPE, HDPE and PP)

3.1.1 Physical measurements

Table 1 outlines all of the PW aerogels' measured bulk densities and estimated porosity percentages. Indeed, the development of aerogel phases is supported by low bulk densities and the high porosity percents of all PW aerogels. Remarkably, PW PP aerogel has the lowest bulk density (0.28 mg/cm³) and the highest porosity percentage (99%), suggesting that it is extremely light with ultra-low density. Accordingly, the bulk density values of LDPE and HDPE are higher (0.389 and 0.458 mg/cm³, respectively), and their porosity percentages are lower (85% and 79%). Additionally, Fig. 1 shows how the aerogels' incredibly light weights stick to the leaves of the trees at the Egyptian Petroleum Research Institute. Hence, compared to LDPE and HDPE aerogels, PW PP aerogel retains more air inside its porous structure.

Table 1: Physical and topological properties of derived PW aerogels

| PW aerogel | Bulk density (mg/cm ³) | Porosity (%) | RMS roughness | | WCA (degree) | Water uptake (g) |
|------------|------------------------------------|--------------|---------------|---------|--------------|------------------|
| | | | Ra (nm) | Rq (nm) | | |
| PW LDPE | 0.389 | 85 | 11.2 | 12.9 | 119° | 0 |
| PW HDPE | 0.458 | 79 | 3.5 | 4.2 | 107° | 0 |
| PW PP | 0.028 | 99 | 91.6 | 98.2 | 147.7° | 0 |

3.1.2. Structural and chemical properties

Fig. 2 depicts the XRD patterns of the prepared PW aerogels and their typical diffraction peaks. The developed aerogels vary in their peak intensities, widths, and degrees of crystallinity overall (Table 2). Specifically, compared with PW LDPE and PW PP aerogels, PW HDPE aerogel exhibits sharper and more intense characteristic peaks at 22° and 24° with their crystal planes (110) and (200), respectively [26]. This reveals that PW HDPE has a higher degree of crystallinity, which may be related to its basic structure of fewer hydrocarbon branches (either short or long segments) along the chain polymer skeleton (CH₂-CH₂)_n and more regular molecular packing. An increase in linked side segments along the PE skeleton would result in a decrease in crystalline zones and an increase in amorphous regions. As a result, PW LDPE has more branching side segments, which decrease its crystallinity and expand its amorphous region with the similar diffractions of PW HDPE [20]. In this sense, PW PP aerogel exhibits its characteristic wide peaks with their crystal planes (110), (040), (130), and (111), respectively, at 14, 17, 19, and 21° (Fig. 2) [30]. The high value of the full width at half maximum (FWHM, Table 1) of PW PP diffraction suggests a low crystalline structure and the presence of amorphous zones. It also reveals an aliphatic polypropylene backbone with methyl groups arranged randomly, alternatively, or one sideways. Thus, the crystallinity would be impacted and distinct stereo structures of PP might be involved depending on the irregularity and isotacticity.

Table 2: Structural properties of the derived PW aerogels

| PW aerogel | Position (2θ) | Intensity (%) | Height (cts) | d-spacing (nm) | FWHM | Crystallite size (nm) |
|------------|---------------|---------------|--------------|----------------|-------|-----------------------|
| PW LDPE | 21.7 | 100 | 259 | 0.409 | 0.433 | 19.5 |
| PW HDPE | 22 | 100 | 313.6 | 0.404 | 0.393 | 21.5 |
| PW PP | 13.9 | 100 | 109 | 0.636 | 0.629 | 13.2 |

Moreover, PP polymorphism has a significant role in indicating crystallinity. For instance, quick cooling during synthesis and processing has been shown to inhibit crystallinity to the mesomorphic phase and potentially drop to amorphous PP, although HDPE is not [31]. In turn, structures with irregular molecular packing possibility, like PWPP and PWLDPE, would have less crystalline structures than those with more regular order ability, like PW HDPE. In addition, Fig 2. verifies the semicrystallinity of the entire PW aerogel, exhibiting distinct variations between the crystalline and amorphous zones. Whereas the amorphous portions are made up of randomly oriented polymer chains, the crystalline regions are made up of perfectly oriented crystallographic zones. In spite of this, the Scherrer equation (Table 2) yields the smallest estimated crystallite size for PW PP, indicating well distributed crystallographic polymer chains. On the other hand, PW HDPE has the largest crystallite size, implying that its crystallographic polymer chains have been aggregated.

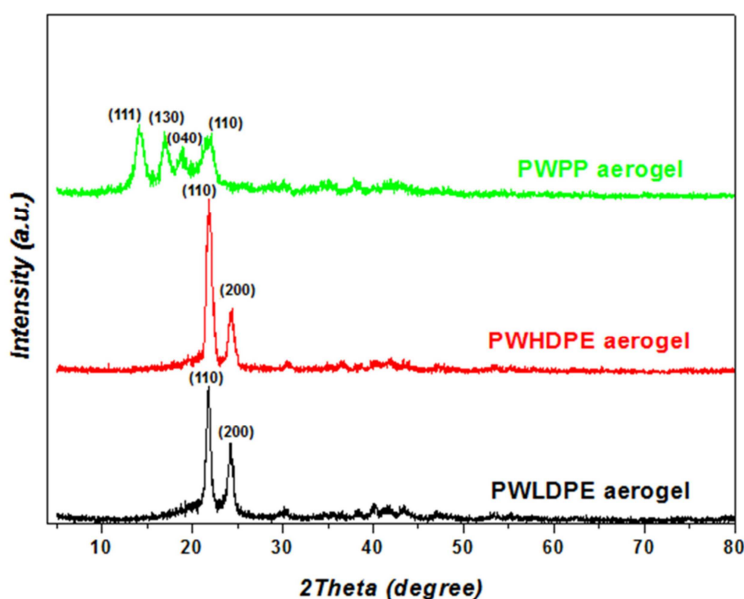


Figure 2: XRD patterns of the prepared PW aerogels

The infrared spectra of the PW aerogels (Fig.3) exhibited stretching frequencies at 2920 and 2850 cm^{-1} characteristic of methylene and methyl groups respectively. PW PP has further peaks at frequencies of 1375, 1164, 979, and 843 cm^{-1} , indicating the presence of its bi-functional group structure consisting of methyl and methylene groups [30]. On the other hand, PW LDPE tends to accommodate both its long and short branching segments throughout its polymer chain (repeating methylene units) due to its methyl group vibrational mode. On the other hand, PW HDPE shows weaker and broader peaks of methylene group vibration modes and an almost entirely absent methyl group vibration mode, which supports the absence of side segments along the repeating methylene polymer backbone (Fig. 3). The absence of polar functional groups like COOH, OH, C=O or NH_2 in the spectra of the three aerogels reflects their hydrophobic nature. Furthermore, it appears that the produced PW aerogels are very chemically stable in all conditions due to the existence of aliphatic polymer chains and the absence of a carbonyl group [32,33].

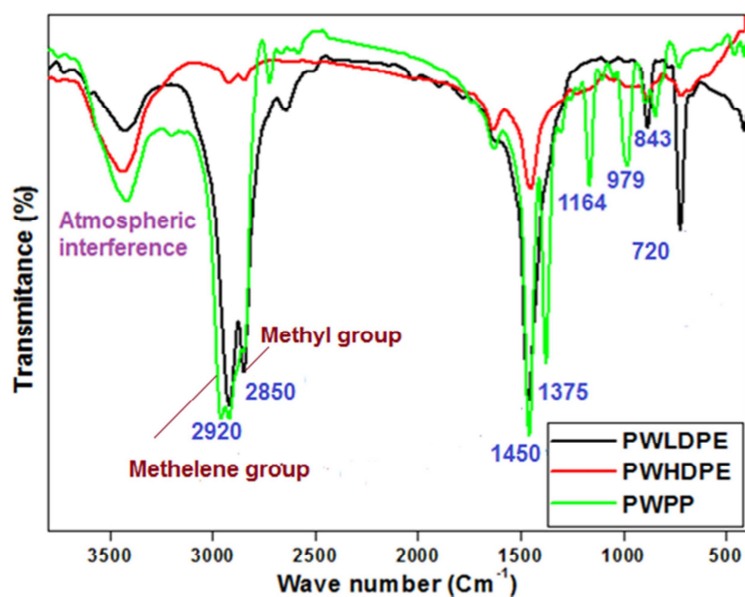


Figure 3: FTIR Spectra for the prepared PW aerogels.

3.1.3. Surface morphology, configuration and topology

Fig. 4 displays the results of the SEM microscopic measurement of morphologies and structural changes of the produced PW aerogels. It's interesting to note that all aerogel have three-dimensional hierarchical surface structures with various morphologies. Moreover, they show comparable degrees of surface roughness and distinct pore configurations. First, Fig. 4a,b shows how the PW LDPE sheets, which resemble petals, are arranged vertically to form a crumbled surface. Additionally, a variety of pore lengths (nano, micro, and macro scales) and the cavities that exist between each set of vertically placed sheets are clearly visible. Comparable micrographs with less distributed pore structure are also seen in PW HDPE because of the presence of both petal-like and fibrous structures (Fig.4c,d). The fibrous structure could negatively impact the textural structure while simultaneously enhancing the mechanical properties [26]. On the other hand, PW PP shows a distinct flower like shape of numerous petals with uniform inter-connected pore structure. Despite the orderly arrangement of petals to create a compatible microscopic floral patterns. The produced flowers appear to be randomly located inside the sample, leading to macro avoids (inter-spaces), and a high degree of porosity and roughness (Fig. 4e,f). Thus, the nature, structure, and kind of PW aerogel would determine the highly porous, crumpled, and rough surface with succeeding pore structure and inter-spaces. As a result, SEM micrographs validate the computed high porosity and extremely low density values of the produced PW aerogels (Table 1).

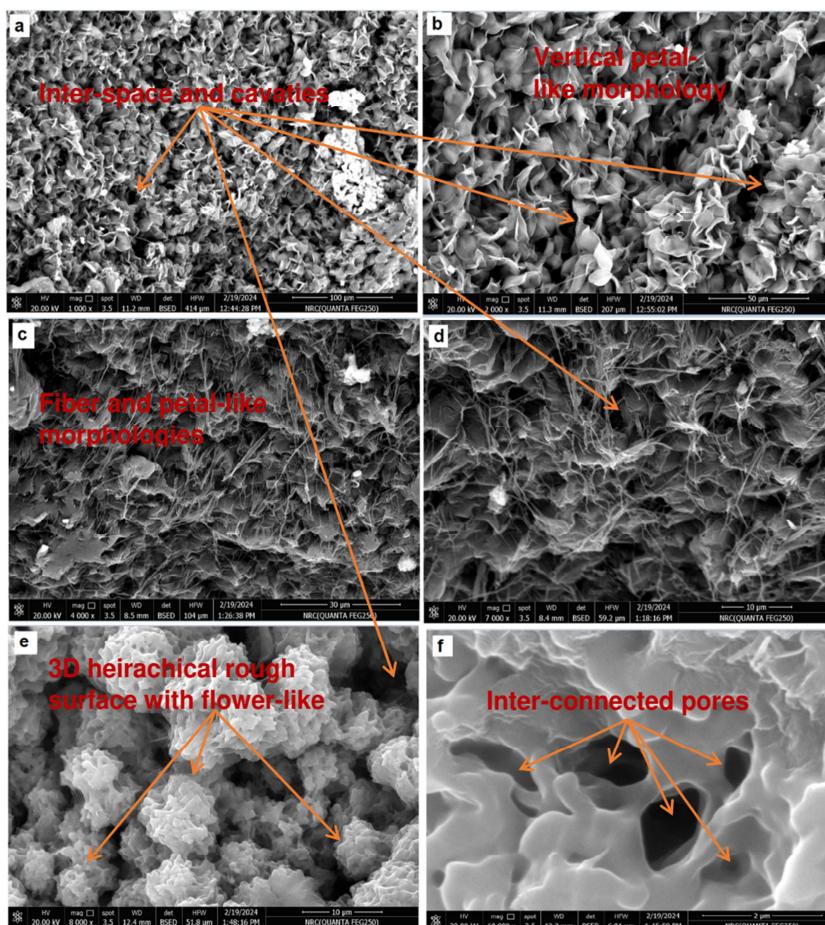


Figure 4: FESEM images for PW aerogels (a and b) PW LDPE, (c and d) PW HDPE, and (e and f) PW PP aerogel.

Figure 5 illustrates the two and three dimensional topographs of each PW aerogels that were acquired by the use of atomic force microscopy (AFM). There are discernibly different levels of smooth and rough surfaces. PW HDPE aerogel has a smoother surface but still has some creases and folds (Fig. 5b). A rougher surface and more zigzags and folds are also present in PW LDPE aerogel compared with PW HDPE aerogel (Fig. 5a). These AFM pictures provide evidence for the lamellar structure of the polymer chains and the presence of shark skin character [32]. It's interesting to note that PW PP has the roughest surface with unique top and bottom surfaces. Based on SEM measurements, these surface tops and bottoms resemble the microstructure of PW PPE flowers and their interspaces (Figs. 5c and 4e). Furthermore, Table 1 displays the variance in the Ra and Rq values for the approximate root mean square (RMS) roughness for PW aerogels top surfaces. PW PP aerogel is capable for exhibiting the highest Ra and Rq values of 91.6 nm and 98.2 nm, respectively, indicating a distinct

rough surface. On the other hand, the extremely low Ra and Rq values of the PW HDPE and PW LDPE aerogels ($Ra_{PW\ HDPE}=3.5\text{nm}$, $Rq_{PW\ HDPE}=4.2\text{nm}$, and $Ra_{PW\ LDPE}=11.2\text{nm}$ and $Rq_{PW\ LDPE}=12.9\text{nm}$) indicate low rough surfaces.

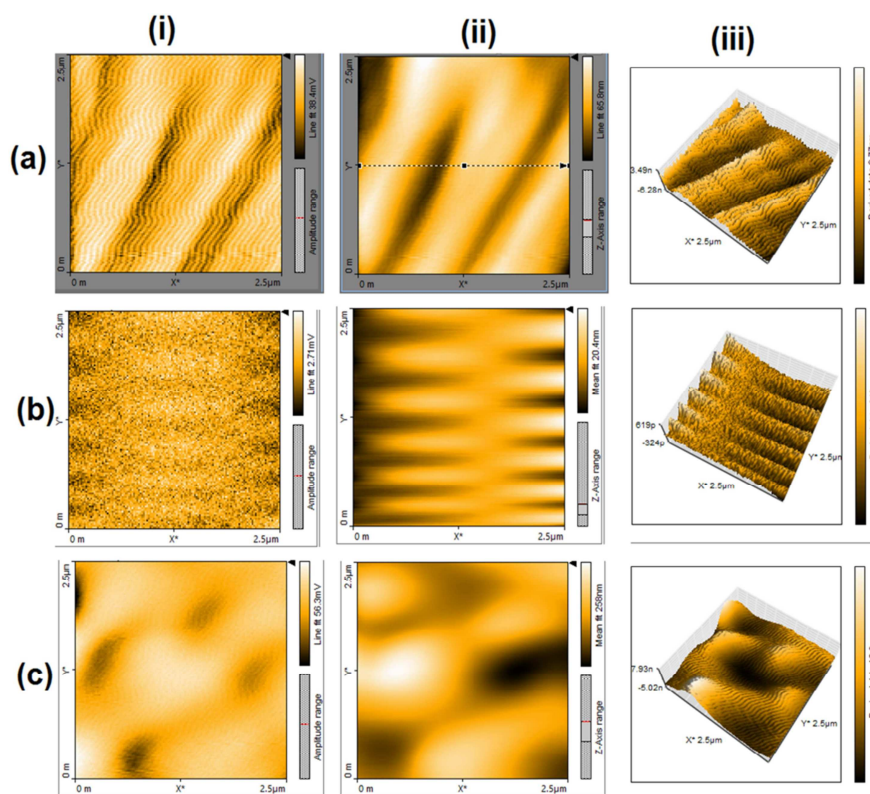


Figure 5: AFM topographs of (a) PW LDPE aerogel, (b) PW HDPE aerogel, and (c) PW PP aerogel; (i) amplitude scan forward, (ii) Z axis scan forward, and (iii) 3 dimensions XYZ axes surface roughness.

3.1.4. Wettability measurements (Hydrophobicity and oleophilicity)

To evaluate the wettability of the developed PW aerogels, the measured WCAs values are displayed in Fig. 6 and Table 2. It is clear that WCA values are in the hydrophobic category ($90^\circ < \text{WCA} < 150^\circ$) [34] due to their aliphatic hydrocarbon structure with nonpolar functional groups (Fig. 3), intrinsic hydrophobicity, highly porous structure, and rough surface of hierarchical microstructure (Figs. 4 and 5) [35]. Furthermore, Table 2 shows that PW PP aerogel has the highest WCA (148°), as well as, the highest porosity, lowest density, and maximum roughness factor. It has also an unusual structure like a three-dimensional flower composed of numerous interconnecting pores and interspace gaps. Therefore, according to Wenzel and Cassie-Baxter models [29], air trapping inside the hieracial microstructure rough surface, highly interconnected pores, and interspace cavities could explain the exceptionally hydrophobic character of PWPP aerogel. These superhydrophobic air groves would trap excess air and prevent water droplets from dispersing over the PW PP surface. Even without any organic-inorganic driven superhydrophobicity ($150^\circ < \text{WCA} < 180^\circ$) [29,34,35], PW PP remarkably displays a comparable WCA value (148°). This indicates that the WCA values of PW LDPE and PW HDE aerogels are lower than those of PW PP aerogel. Because HDPE aerogel tends to form more crystalline structures with regular polymer chain packing (Fig. 2), less porosity, and a roughness factor (Table 2, Fig 5), it would have fewer air groves and a lower WCA value (Fig. 6). PW LDPE aerogel has more branching structure, an unorganized packing tendency, a higher roughness factor, and a more porous structure (Fig. 4) that functions as an air groove with a higher WCA value than PW HDPE aerogels.

In practical terms, Fig. 6 indicates that all of the PW aerogels are water-repellents. With no discernible sorption or wide-spread volume, the water droplets remain stacked on their surface. In addition, for a week, all of the PW aerogel samples that were submerged in water in a second practical investigation floated on the water's surface without absorbing any water because they didn't gain any weight (Table 2). The wetting behavior of PW aerogels, particularly PW PP aerogel, thus resembles that of naturally occurring superhydrophobic surfaces, such as lotuses, shark skin, etc. (Fig. 6), suggesting both the easy to self clean and water repellent properties of the derived PW aerogels. In contrast, Fig. 6 illustrates how extensively distributed the oil droplet is across the PW aerogel surfaces, indicating the high sorption affinity of PW aerogels for the oil droplets. As a result, the produced PW aerogels show attractive long-term water repellency and oleophilicity properties.



Figure 6: Wettability of the prepared PW aerogels and the natural super hydrophobic surfaces.

3.2 Oil uptake efficiency

Fig. 7 illustrates the sorption capacities and removal efficiencies of the produced PW aerogels toward lubricating, diesel, and crude oil. Clearly, PW PP aerogels effectively absorb several kinds of oil, such as lubricating oil, diesel oil, and crude oil (Fig.7). On the other hand, neither PW LDPE nor PW HDPE could completely remove oil from water (Fig. 7). What's more intriguing is that every PW aerogels exhibits distinct oil absorption capacities and efficiencies for every type of oil. Because PW PP aerogel combines surface adhesion, capillary action [36-38], adsorption, absorption, and cohesion [5], it has the best sorption capacities and removal efficiency of all oil types (Fig. 7). Due to differences in their viscosities, it also absorbs diesel oil more effectively than lubricating and crude oil [39]. Table 2 shows that PW PP has the largest porosity of 99% and the highest air volume density, both of which improve oil sorption efficiency. Furthermore, its structure is very porous, exhibiting a range of pore sizes and pore geometries (Fig. 4e and f). It is convenient to absorb viscous liquids like crude oil due to its large pores size [40,41]. On the other hand, the interconnected pores in the nanoscale serve as pore channels that allow the capillary force to drive the oil inside the PW PP aerogel.

As a result, oil would simply penetrate the pores or capillary channels [42]. PW PP aerogel's sorption capacity is increased by these narrow pores since they likewise sorb oil at a quicker rate than larger pores. [43]. Additionally, PW PP aerogel may swell oil better due to its three-dimensional structure (Fig. 4) [44]. As a result, the micro hierarchical surface structure of the PW PP (Fig. 4) reveals a rougher surface (Table 2), on which more oil adheres and sticks [45,46]. The most notable benefit of the rougher surface of PW PP aerogel is that it would pull in more oil and repel water more effectively, increasing its sorption capacity and removal efficiency [47]. This is consistent with the AFM topographs (Fig. 5) and the largest WCA of PW PP (Fig. 6). In contrast, PW HDPE shows limited removal efficiency and sorption capacity for all oil types (Fig. 7). As a result, it shares a common flaw in regard to its design and functionality. Particularly, PW HDPE has the lowest pore structure with larger interspace cavities that have rapidly become saturated with small quantities of oil because of its higher crystallinity, smoother surface, smaller WCA, compact structure, and low porosity. Further oil would not be absorbed into the PWHDE aerogel once it has been saturated with these little amounts of oil [36]. Consequently, the inadequate structure of PW HDPE aerogel prevents oil from spreading and permeating it. The more favorable structure of the PW LDPE aerogel (Fig. 4 a and b) allows it to repel water and absorb oil selectively, resulting in better performance than the PW HDPE aerogel. The decreased sorption capacities and removal efficiencies for both PW HDPE and PW LDPE may be related to the absence of capillary action in oil uptake operation due to the lack of smaller pore sizes, as shown by SEM (Fig. 4). Additionally, the surfaces of both of them (Table 2 and Fig. 5) are less rough, which decrease the ability of oil to stick to them. They have a smaller degree of porosity in this regard (Table 2), which limits the amount of sorbed oil inside their structure because they would only be saturated with a certain amount of oil. Additionally, they show reduced WCAs (Table 2), which is essential for increased removal efficiency and sorption capacity.

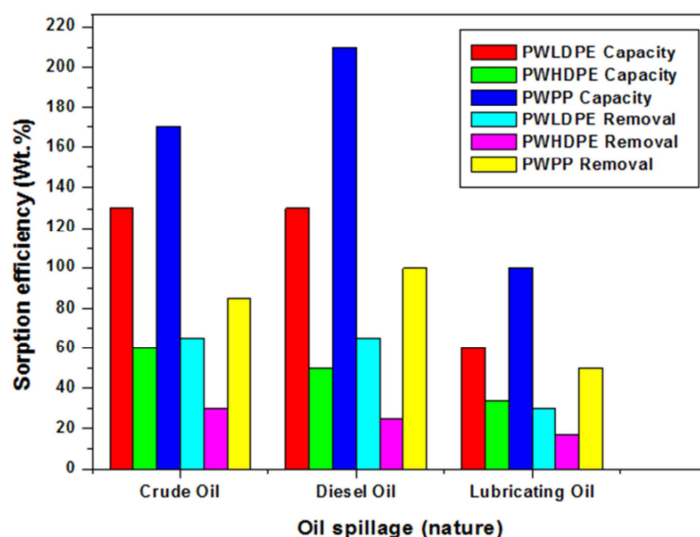


Figure7: Sorption capacities and removal efficiencies of PW aerogels toward different oil derivatives.

Table 3 shows the physical properties of lubricating oil, diesel oil, and crude oil. It has been noted that highly viscous oils are very difficult to absorb across sorbents [36]. Lubricating oil has a stronger cohesive force than other oil slicks since it is rationally more viscous than crude oil and diesel oil. Thus, following the sorption test, a lower amount of oil is expected to drip. Following a sorption test, cohesion, adhesion, and gravimetric forces determine how much oil drains from the aerogel sorbent [47]. Diesel oil, on the other hand, would absorb more readily within the PW aerogels and may leak more after the sorption test. Diesel oil has the maximum sorption capacity and removal efficiency for each PW aerogel, as demonstrated in Figs. 7 and 8, making it easier to be sorbed over the full PW aerogel than the other oils investigated. It comes out that crude oil is absorbed over all PW aerogels more efficiently than lubricating oil due to variation in their viscosities (Fig. 7). Furthermore, it might be related to the impact of additives in lubricating oils, which have lowered the sorption rate and altered the sorption equilibrium [48].

Table 3: Physical characteristics of various oil

| Oil/Test | Crude oil | Diesel oil | Lubricating oil |
|------------------------------------|-----------|----------------|-----------------|
| Viscosity (40°C, Cst) | 13.6 | 0.2991 | 150.43 |
| Density (15°C, g/Cm ³) | 0.9150 | 0.7618 | 0.8906 |
| Specific gravity (API) | 0.9159 | 0.7625 | 0.8915 |
| Pour point (°C) | 12 | Less than - 45 | -12 |

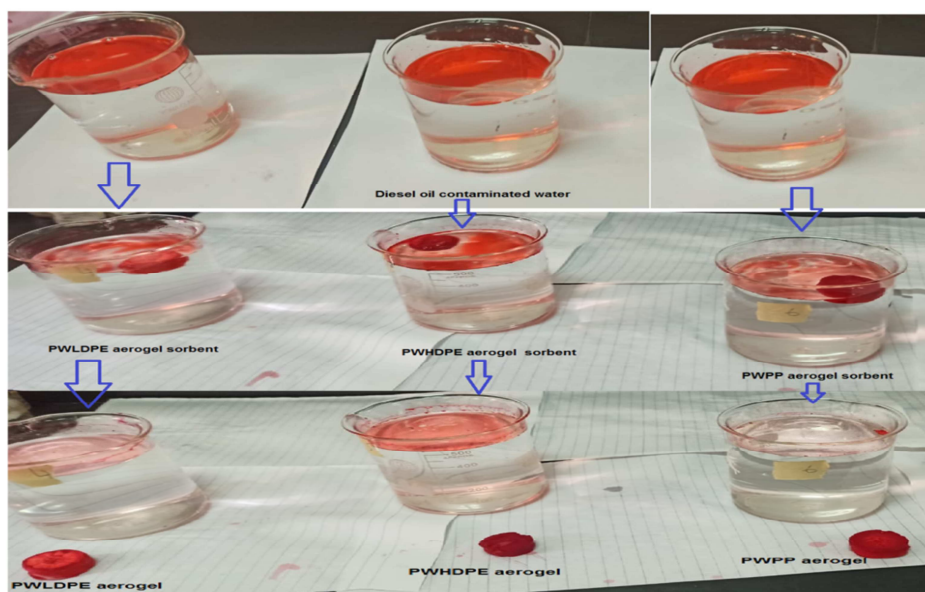


Figure 8: Practical sequence of diesel oil removal by PW aerogels.

3.3 Structural durability, resuability and regeneration

Reusing the spent PW aerogels involves washing them with n-hexane to remove any leftover oil and drying them at 80°C. Fig. 9 illustrates how fully developed PW aerogels can be reused eight times with diesel oil. Remarkably, the only wasted PW PP aerogel exhibits high stable removal effectiveness (99%) of diesel oil for six cycles before declining to 30%. After each cycle, about 100% of the sorbed diesel oil may be extracted from the wasted PW PP aerogel and used again with the same level of efficiency. Conversely, in subsequent cycles, the removal efficiencies of both wasted PW HDPE and PW LDPE aerogels exhibited a significant decline. As a result, after the regeneration process, they retain and trap part of the diesel oil. After every cycle, it is therefore challenging to completely remove the sorbed diesel oil from their structure. The oil that has become trapped in their cavities and pores prevents more oil to be absorbed during the next cycle.

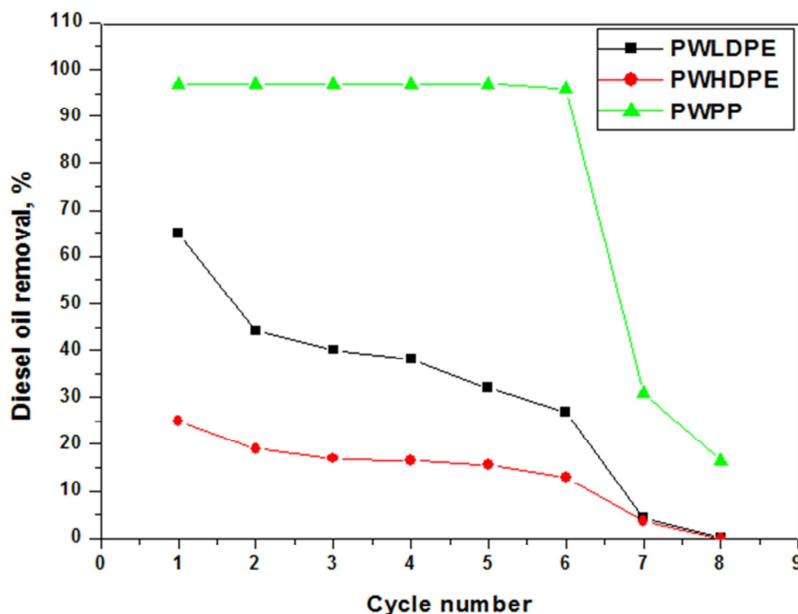


Figure 9: Reusability of PW aerogels toward diesel oil sorption.

Specifically, Fig. 10 delves more into the oil recovery and cyclic stability of wasted PW PP aerogel. Notably, steady, high sorption capacity and complete oil recovery are achieved during multiple cycles of sorption capability. PW PP aerogels hence showed stable sorption releasing oil cycles. Above all, the final spent PW PP aerogels would not be discarded since it lacked the stable sorption-releasing oil cycles property.

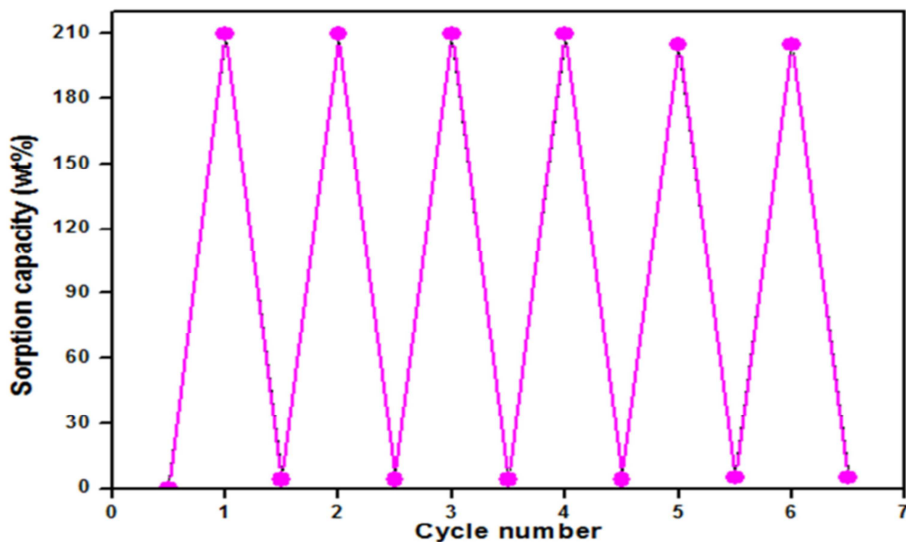


Figure 10: Sorption desorption cycle stability of PW PP toward diesel oil.

To recycle and restore them, the PW aerogels experimental preparation process would be applied (Fig. 1). For long-term use, PW PP aerogel can therefore be utilized indefinitely. Furthermore, because PW aerogels show no signs of structural failure after each cycle, they have excellent mechanical toughness and outstanding structural longevity. To ascertain the utilization of the developed PW aerogels, Table 4 outlined the sorption capacities of other sorbents and compared them to our work.

Table 4: Comparative studies of different sorbents.

| Material | Sorption capacity or removal efficiency | Reference |
|--------------------|---|-----------|
| Cogon grass | 93.53% | [49] |
| Palm-oil shells | 98% | [50] |
| Corn stalk pith | 44.1 g/g | [51] |
| Banana peel | 6.35 g/g | [52] |
| sugar-cane bagasse | 70–80% | [53] |
| LDPE | 3.4g/g | [20] |
| PWPP | 99% | Our work |
| PWLDPE | 65% | Our work |
| PWHDPE | 25% | Our work |

4. Conclusions

PW aerogels, such as PW LDPE, PW HDPE, and PW PP, are easily generated using a cyclic eco-preparation technique. Physical, structural, and chemical properties, surface morphologies, and topologies, and wetting behavior of the developed PW aerogels are described. The target of preparing these aerogels is to investigate, illustrate, and compare the effectiveness of these materials for treating oily contaminated water. PW PP aerogel is remarkably highly porous, with a wide range of pore sizes and geometries; it also has a rough, three-dimensional surface with a rough texture like flowers; it has the largest air content; it has ultralight weight; and its bulk density is lowest. A smoother surface, fewer side chain segments, a lower WCA, a higher bulk density, a reduced porosity with macropores and interspace cavities, and a more flowless crystalline structure with regular polymer chain. In comparison with PW HDPE, PW LDPE exhibits a rougher surface with a vertical petal-like arrangement, a larger WCA, a lower bulk density, more air grooves, a more porous structure, and further side segments that obstruct proper packing. The generated PW aerogel is used to sorb several types of oils, including lubricating oil, diesel, and crude oil. Because of its outstanding physical, structural, surface, and wetting qualities, PWPP aerogel rationally shows the maximum sorption capacity and removal efficiency toward the three oils. Furthermore, compared with others, it performs better over the course of seven sorption-desorption cycles. Conversely, because of its inconvenient properties, PWHDPE is the lowest sorption capacity and removal efficiency for sorbing all the three types of oil. Furthermore, PW LDPE aerogel is more effective than PW HDPE aerogel due to its superior attributes. Additionally, the influence of formulation factors (additives) and physical characteristics of oil (viscosity, in particular) on the overall sorption efficiency is considered. Viscous oils, like heavy oil, are harder to sorb than diesel oil and have lower sorption capacities for all PW aerogel sorbents. However, because lubricating oil contains additives that alter the sorption rate and equilibrium, it showed lower sorption capacities than crude oil for all PW aerogels.

Fund

The authors have no fund

Conflict of Interests

The authors declare that they have no known competing financial interests or personal relationships that could have appeared to influence the work reported in this manuscript.

Acknowledgment

The authors are gratefully grateful to acknowledge

The Egyptian Petroleum Research Institute and the Faculty of Science, Ain shams University.

5. References

- [1] Ganesamoorthy, R., Vadivel, V. K., Kumar, R., Kushwaha, O. S., & Mamane, H. (2021). Aerogels for water treatment: A review. *Journal of Cleaner Production*, 329, 129713.
- [2] Torres, C. E. I., Quezada, T. E. S., Kharissova, O. V., Kharisov, B. I., & de la Fuente, M. I. G. (2021). Carbon-based aerogels and xerogels: Synthesis, properties, oil sorption capacities, and DFT simulations. *Journal of Environmental Chemical Engineering*, 9(1), 104886.
- [3] Oliveira, L. M., Saleem, J., Bazargan, A., Duarte, J. L. D. S., McKay, G., & Meili, L. (2021). Sorption as a rapidly response for oil spill accidents: A material and mechanistic approach. *Journal of Hazardous Materials*, 407, 124842.
- [4] Emenike, E. C., Adeleke, J., Iwuozor, K. O., Ogunniyi, S., Adeyanju, C. A., Amusa, V. T., ... & Adeniyi, A. G. (2022). Adsorption of crude oil from aqueous solution: a review. *Journal of Water Process Engineering*, 50, 103330.
- [5] Saleem, J., Riaz, M. A., & Gordon, M. (2018). Oil sorbents from plastic wastes and polymers: A review. *Journal of hazardous materials*, 341, 424-437.

- [6] Paulauskienė, T., Jucikė, I., Juščenko, N., & Baziukė, D. (2014). The use of natural sorbents for spilled crude oil and diesel cleanup from the water surface. *Water, Air, & Soil Pollution*, 225, 1-12.
- [7] Akpomie, K. G., & Conradie, J. (2021). Enhanced surface properties, hydrophobicity, and sorption behavior of ZnO nanoparticle-impregnated biomass support for oil spill treatment. *Environmental Science and Pollution Research*, 28(20), 25283-25299.
- [8] Kundu, P., & Mishra, I. M. (2018). Treatment and reclamation of hydrocarbon-bearing oily wastewater as a hazardous pollutant by different processes and technologies: a state-of-the-art review. *Reviews in Chemical Engineering*, 35(1), 73-108.
- [9] Zamparas, M., Tzivras, D., Dracopoulos, V., & Ioannides, T. (2020). Application of sorbents for oil spill cleanup focusing on natural-based modified materials: A review. *Molecules*, 25(19), 4522.
- [10] Ani, J. U., Akpomie, K. G., Okoro, U. C., Aneke, L. E., Onukwuli, O. D., & Ujam, O. T. (2020). Potentials of activated carbon produced from biomass materials for sequestration of dyes, heavy metals, and crude oil components from aqueous environment. *Applied Water Science*, 10, 1-11.
- [11] Kukkar, D., Rani, A., Kumar, V., Younis, S. A., Zhang, M., Lee, S.-S Lee Tsang D.C. & Kim, K. H. (2020). Recent advances in carbon nanotube sponge-based sorption technologies for mitigation of marine oil spills. *Journal of Colloid and Interface Science*, 570, 411-422.
- [12] Torres, C. E. I., Quezada, T. E. S., Kharissova, O. V., Kharisov, B. I., & de la Fuente, M. I. G. (2021). Carbon-based aerogels and xerogels: Synthesis, properties, oil sorption capacities, and DFT simulations. *Journal of Environmental Chemical Engineering*, 9(1), 104886.
- [13] Shahmirzaee, M., Hemmati-Sarapardeh, A., Husein, M. M., Schaffie, M., & Ranjbar, M. (2019). A review on zeolitic imidazolate frameworks use for crude oil spills cleanup. *Advances in Geo-Energy Research*, 3(3), 320-342.
- [14] ben Hammouda, S., Chen, Z., An, C., & Lee, K. (2021). Recent advances in developing cellulosic sorbent materials for oil spill cleanup: A state-of-the-art review. *Journal of Cleaner Production*, 311, 127630.
- [15] Peng, D., Ouyang, F., Liang, X., Guo, X., Dang, Z., & Zheng, L. (2018). Sorption of crude oil by enzyme-modified corn stalk vs. chemically treated corn stalk. *Journal of Molecular Liquids*, 255, 324-332.
- [16] Emenike, E. C., Iwuozor, K. O., Agbana, S. A., Otoikhian, K. S., & Adeniyi, A. G. (2022). Efficient recycling of disposable face masks via co-carbonization with waste biomass: a pathway to a cleaner environment. *Cleaner Environmental Systems*, 6, 100094.
- [17] Omer, A. M., Khalifa, R. E., Tamer, T. M., Ali, A. A., Ammar, Y. A., & Eldin, M. M. (2020). Kinetic and thermodynamic studies for the sorptive removal of crude oil spills using a low-cost chitosan-poly (butyl acrylate) grafted copolymer. *Desalin. Water Treat*, 192, 213-225.
- [18] Emenike, E. C., Adeniyi, A. G., Omuku, P. E., Okwu, K. C., & Iwuozor, K. O. (2022). Recent advances in nano-adsorbents for the sequestration of copper from water. *Journal of Water Process Engineering*, 47, 102715.
- [19] Medjahdi, M., Benderdouche, N., Bestani, B., Duclaux, L., & Reinert, L. (2016). Modeling of the sorption of crude oil on a polyurethane foam-powdered activated carbon composite. *Desalination and Water Treatment*, 57(47), 22311-22320.
- [20] Bera, T., Manna, S., Sharma, A. K., Bahukhandi, K., Sharma, M., & Bhunia, B. (2023). Repurposing the single-used-plastic for development of hydrophobic aerogels for remediation of oil spill and organic solvents. *Science of The Total Environment*, 903, 166670.
- [21] Saleem, J., Moghal, Z. K. B., & McKay, G. (2023). Designing super-fast trimodal sponges using recycled polypropylene for organics cleanup. *Scientific Reports*, 13(1), 14163.
- [22] Saleem, J., Moghal, Z. K. B., Sun, L., & McKay, G. (2024). Valorization of mixed plastics waste for the synthesis of flexible superhydrophobic films. *Advanced Composites and Hybrid Materials*, 7(1), 11.
- [23] Daniel, C., Longo, S., & Guerra, G. (2015). High porosity polyethylene aerogels.
- [24] Zou, L., Phule, A. D., Sun, Y., Zhu, T. Y., Wen, S., & Zhang, Z. X. (2020). Superhydrophobic and superoleophilic polyethylene aerogel coated natural rubber latex foam for oil-water separation application. *Polymer Testing*, 85, 106451.
- [25] Saleem, J., & McKay, G. (2016). Waste HDPE bottles for selective oil sorption. *Asia-Pacific Journal of Chemical Engineering*, 11(4), 642-645.
- [26] Gan, L., Zhang, D., Yue, X., Xu, J., Qiu, F., & Zhang, T. (2022). A recyclable and regenerated aerogel membrane derived from waste plastic for emulsion separation. *Journal of Environmental Chemical Engineering*, 10(5), 108221.
- [27] Saleem, J., Ning, C., Barford, J., & McKay, G. (2015). Combating oil spill problem using plastic waste. *waste management*, 44, 34-38.
- [28] Lang, X. H., Zhu, T. Y., Zou, L., Prakashan, K., & Zhang, Z. X. (2019). Fabrication and characterization of polypropylene aerogel material and aerogel coated hybrid materials for oil-water separation applications. *Progress in Organic Coatings*, 137, 105370.
- [29] Do, N. H., Nguyen, T. H., Pham, B. T., Nguyen, P. T., Nguyen, S. T., Duong, H. M., & Le, P. K. (2021). Green fabrication of flexible aerogels from polypropylene fibers for heat insulation and oil/water separation. *Journal of Porous Materials*, 28, 617-627.
- [30] Choi, H., Parale, V. G., Lee, K. Y., Nah, H. Y., Driss, Z., Driss, D., Bouabidi, A., Euchy, S., & Park, H. H. (2019). Polypropylene/silica aerogel composite incorporating a conformal coating of methyltrimethoxysilane-based aerogel. *Journal of nanoscience and nanotechnology*, 19(3), 1376-1381.
- [31] PW2 Mileva, D., Androsch, R., Cavallo, D., Alfonso, G.C. (2012). *European Polymer Journal* 48, 1082-1092.
- [32] Ronca, S. (2017). Polyethylene. In *Brydson's plastics materials* (pp. 247-278). Butterworth-Heinemann.

- [33] Gahleitner, M., & Paulik, C. (2017). Polypropylene and other polyolefins. In *Brydson's plastics materials* (pp. 279-309). Butterworth-Heinemann.
- [34] Jishnu, A., Jayan, J. S., Saritha, A., Sethulekshmi, A. S., & Venu, G. (2020). Superhydrophobic graphene-based materials with self-cleaning and anticorrosion performance: An appraisal of neoteric advancement and future perspectives. *Colloids and Surfaces A: Physicochemical and Engineering Aspects*, 606, 125395.
- [35] Chen, Z., Dong, L., Yang, D., & Lu, H. (2013). Superhydrophobic graphene-based materials: surface construction and functional applications.
- [36] Hoang, A. T., Nižetić, S., Duong, X. Q., Rowinski, L., & Nguyen, X. P. (2021). Advanced super-hydrophobic polymer-based porous absorbents for the treatment of oil-polluted water. *Chemosphere*, 277, 130274.
- [37] Diersch, H. J. G., Clausnitzer, V., Myrnyy, V., Rosati, R., Schmidt, M., Beruda, H., & Virgilio, R. (2010). Modeling unsaturated flow in absorbent swelling porous media: Part 1. Theory. *Transport in Porous Media*, 83, 437-464.
- [38] Masoodi, R., Tan, H., & Pillai, K. M. (2011). Darcy's law-based numerical simulation for modeling 3D liquid absorption into porous wicks. *AIChE journal*, 57(5), 1132-1143.
- [39] Hoang, A. T., Nižetić, S., Duong, X. Q., Rowinski, L., & Nguyen, X. P. (2021). Advanced super-hydrophobic polymer-based porous absorbents for the treatment of oil-polluted water. *Chemosphere*, 277, 130274.
- [40] Ribeiro, T. H., Smith, R. W., & Rubio, J. (2000). Sorption of oils by the nonliving biomass of a *Salvinia* sp. *Environmental Science & Technology*, 34(24), 5201-5205.
- [41] Browsers, S. D. (1982). Understanding sorbents for cleaning up spills. *Plant Eng*, 3, 219-221.
- [42] Washburn, E. W. (1921). The dynamics of capillary flow. *Physical review*, 17(3), 273.
- [43] Brugnara, M. A. R. C. O., Della Volpe, C. L. A. U. D. I. O., Maniglio, D., Siboni, S., Negri, M., & Gaeti, N. (2006). Wettability of porous materials. I: The use of Wilhelmy experiment: The cases of stone, wood and non-woven fabric. *Contact angle, wettability and adhesion*, 4, 115-141.
- [44] Marsh Jr, H. E. (1977). Oil and fat absorbing polymers.
- [45] Jin, Y., Jiang, P., Ke, Q., Cheng, F., Zhu, Y., & Zhang, Y. (2015). Superhydrophobic and superoleophilic polydimethylsiloxane-coated cotton for oil-water separation process: an evidence of the relationship between its loading capacity and oil absorption ability. *Journal of hazardous materials*, 300, 175-181.
- [46] Moreno, M. C., Brown, C. A., & Bouchon, P. (2010). Effect of food surface roughness on oil uptake by deep-fat fried products. *Journal of Food Engineering*, 101(2), 179-186.
- [47] Saleem, J., Moghal, Z. K. B., & McKay, G. (2023). 3D Oleophilic Sorbent Films Based on Recycled Low-Density Polyethylene. *Polymers*, 16(1), 135. <https://doi.org/10.3390/polym16010135>
- [48] Mishra, P. K., & Mukherji, S. (2012). Biosorption of diesel and lubricating oil on algal biomass. *3 Biotech*, 2, 301-310.
- [49] Khalid, F. E., Ahmad, S. A., Zakaria, N. N., Shaharuddin, N. A., Sabri, S., Azmi, A. A., Khalil, K. A., Verasoundarapandian, G., Gomez-Fuentes, C., & Zulkharnain, A. (2021). Application of cogon grass (*Imperata cylindrica*) as biosorbent in diesel-filter system for oil spill removal. *Agronomy*, 11(11), 2273. <https://doi.org/10.3390/AGRON11112273>.
- [50] Sahu, J. N., Karri, R. R., & Jayakumar, N. S. (2021). Improvement in phenol adsorption capacity on eco-friendly biosorbent derived from waste Palm-oil shells using optimized parametric modelling of isotherms and kinetics by differential evolution. *Industrial Crops and Products*, 164, 113333. <https://doi.org/10.1016/J.INDCR.2021.113333>.
- [51] Peng, D., Cheng, S., Li, H., & Guo, X. (2021). Effective multi-functional biosorbent derived from corn stalk pith for dyes and oils removal. *Chemosphere*, 272, 129963. <https://doi.org/10.1016/J.CHEMOSPHERE.2021.129963>.
- [52] Alaa El-Din, G., Amer, A. A., Malsh, G., & Hussein, M. (2018). Study on the use of banana peels for oil spill removal. *Alexandria Engineering Journal*, 57(3), 2061-2068. <https://doi.org/10.1016/J.AEJ.2017.05.020>.
- [53] Anusha, Y G · Avryl Anna Machado · Lavanya Mulky, A Comparative Study of Treatment Methods of Raw Sugarcane Bagasse for Adsorption of Oil and DieselWater Air Soil Pollut (2023) 234:21